https://doi.org/10.5194/egusphere-2023-2451
Preprint. Discussion started: 17 November 2023

Mapping geodetically inferred Antarctic ice height changes into thickness variations: a sensitivity study

Natasha Valencic[1], Linda Pan[1], Konstantin Latychev[2], Natalya Gomez[3], Evelyn Powell[4], and Jerry X Mitrovica[1]

[1]Department of Earth and Planetary Sciences, Harvard University, USA
[2]SEAKON, Toronto, Canada
[3]Department of Earth and Planetary Sciences, McGill University, Canada
[4]Department of Earth and Environmental Sciences, Columbia University, USA

Correspondence: Natasha Valencic (natashavalencic@g.harvard.edu)

Abstract. Determining recent Antarctic ice volume changes from satellite altimeter measurements of ice height requires a correction for contemporaneous vertical crustal deformation. This correction must consider two main sources of crustal deformation: (1) ongoing glacial isostatic adjustment (GIA), that is, the deformational, gravitational and rotational response to late Pleistocene and Holocene ice and ocean mass changes; and (2) modern ice mass flux. In this study, we seek to quantify the uncertainties associated with each of these corrections. Corrections of ice height changes for (1) have generally involved the adoption of global models of GIA defined by some preferred combination of ice history and mantle viscoelastic structure. We have computed the GIA correction generated from a coupled ice sheet - sea level model and a realistic earth model incorporating three-dimensional viscoelastic structure. Integrating the difference between this correction and those from recent GIA analyses widely adopted in the literature yields an uncertainty in total present-day ice volume change equivalent to approximately 10% of Antarctic ice mass loss inferred for the previous decade. This reinforces earlier work indicating that ice histories characterized by relatively high excess ice volume at the Last Glacial Maximum may be introducing significant error in estimates of modern melt rates. Regarding correction (2), a spatially invariant scaling has commonly been used to convert GIA-corrected ice height changes obtained from satellite altimetry into ice volume estimates. We adopt modeling results based on a projection of Antarctic ice mass flux over the next 40 years to demonstrate a spatial variability in the scaling of up to 10% across the ice sheet. Furthermore, using these calculations, we find an error in the projected net ice volume change of up to 4.5 mm GMSL equivalent forty years after present, with most of the difference arising in areas of West Antarctica above mantle zones of low viscosity.

1 Introduction

Modern satellite measurements of ice volume are critical to estimates of global sea level change. Geodetic systems such as the Geoscience Laser Altimetry System aboard the Ice, Cloud, and Land Elevation Satellite (ICESat) measure changes in the height of the ice surface over time. To convert these measurements of surface elevation (henceforth referred to as ice height) into estimates of ice mass, several corrections must be applied. A "firn correction" is necessary, which is based on information

https://doi.org/10.5194/egusphere-2023-2451
Preprint. Discussion started: 17 November 2023

regarding the density and thickness of ice-firn layers. Corrections are also required for crustal elevation changes due to both glacial isostatic adjustment (GIA) and the response to modern-day melt (Groh et al., 2012).

GIA represents the ongoing deformational, gravitational, and rotational response of the Earth to the ice/open-ocean mass transfer across the Pleistocene glacial cycles and into the Holocene (Mitrovica and Milne, 2002). Model-based corrections of altimeter data for GIA require constraints on ice history and mantle viscoelastic structure. Uncertainties in either of these will propagate forward and result in uncertainties in estimates of ice thickness change. Ice histories are commonly inferred by fitting GIA models to sea level datasets in both the near- and far-field of ice sheets (Lambeck et al., 2014; Peltier et al., 2015). Ice sheet modeling, either in combination with GIA modeling or as a standalone approach, can also be used to constrain ice history (Whitehouse et al., 2012; Gomez et al., 2013, 2018). Mantle viscosity fields have been implemented in GIA modeling at various levels of complexity. One-dimensional models assume that the viscosity of the mantle depends only on depth (Lambeck et al., 2014; Peltier et al., 2015), while their more computationally expensive three-dimensional counterparts include lateral variation in the mantle viscosity (Li et al., 2020). This complexity is advisable when modeling GIA in the Antarctic region due to large variations in lithospheric thickness and viscosity beneath the continent. Notably, the mantle beneath parts of West Antarctica is several orders of magnitude less viscous than under East Antarctica (Powell et al., 2020) and lithospheric thickness increases by as much as a factor $\sim$4 from West to East Antarctica.

Correcting altimeter data for crustal deformation due to modern-day melting is generally based on elastic one-dimensional Earth models. In this case, elastic Love number theory (Farrell and Clark, 1976) has been applied to approximate the ratio of ice thickness to surface elevation changes. In previous work, this ratio was fixed at a value of $\alpha = 1.0205$ by considering the average spatial scale of various Antarctic drainage basins (Groh et al., 2012). However, the full expression for the scaling derived from Love number theory indicates the ratio is dependent on spatial scale and will thus be geographically variable (see the theory section). Moreover, given the low mantle viscosity below parts of Antarctica, viscous effects may also impact the relationship between ice height and thickness changes over time scales of a few decades (Powell et al., 2020).

In this article, we seek to quantify the level of uncertainty in ice volume estimates derived from altimetry data introduced by uncertainties in the treatment of GIA and crustal deformation due to modern melting. The next section summarizes the Love-number-based mapping between ice height and thickness changes. The following results section has two parts. First, we use published models to quantify the range of GIA corrections for ongoing crustal uplift in Antarctica. Next, we generate a crustal uplift field from a published projection of Antarctic ice evolution in the 21$^{\text{st}}$ century and use this field as a synthetic data set to explore the geographically variable mapping between ice height and thickness changes in response to modern ice mass flux.

2 Theory

Following the discussion in Groh et al. (2012), we begin with the spherical-harmonic formulation of the sea level equation on a one-dimensional elastic Earth. The global sea level change at colatitude θ and east longitude ϕ, $\Delta SL(\theta, \phi)$, is given by Kendall

https://doi.org/10.5194/egusphere-2023-2451
Preprint. Discussion started: 17 November 2023

et al. (2005) as

$$\Delta SL(\theta,\phi) = \frac{4\pi a^3}{M_e}\sum_{\ell=0}^{\infty}\sum_{m=-\ell}^{\ell}[\rho_i \Delta I_{\ell m} + \rho_w \Delta S_{\ell m}] T_\ell E_\ell Y_{\ell m}(\theta,\phi) \tag{1}$$

where a and M_e are the radius and mass of the Earth while ρ_i and ρ_w are the densities of ice and water. ΔI and ΔS are the spherical-harmonic coefficients of degree ℓ and order m of ice height change and ocean height change, respectively. These are associated with the basis functions $Y_{\ell m}$, which are normalized in our calculations such that

$$\iint_{\Omega} Y_{\ell m}(\theta,\phi) Y^*_{\ell' m'}(\theta,\phi) d\theta d\phi = 4\pi \delta_{\ell\ell'}\delta_{mm'} \tag{2}$$

where the asterisk denotes complex conjugation. Furthermore,

$$T_\ell = \frac{1}{2\ell+1} \text{ and } E_\ell = 1 + k_\ell - h_\ell \tag{3}$$

In the latter equation, k_ℓ and h_ℓ are elastic Love numbers that govern perturbations in the gravitational potential and crustal elevation, respectively. The unity term in the definition of E_ℓ represents the direct gravitational potential perturbation due to load redistribution. The global sea level change is given by the difference in perturbations to the sea surface and crustal elevations. The latter can be isolated from Equation 1 to obtain

$$\Delta R(\theta,\phi) = \frac{4\pi a^3}{M_e}\sum_{\ell=0}^{\infty}\sum_{m=-\ell}^{\ell}[\rho_i \Delta I_{\ell m} + \rho_w \Delta S_{\ell m}] T_\ell h_\ell Y_{\ell m}(\theta,\phi) \tag{4}$$

One can write an expression for the spherical harmonic coefficients of ice height change as a simple sum of the coefficients of ΔR and ΔI:

$$\Delta H_{\ell m} = \Delta R_{\ell m} + \Delta I_{\ell m} \tag{5}$$

which allows us to express the change in ice thickness ΔI as

$$\Delta I_{\ell m} = \Delta H_{\ell m} - \Delta R_{\ell m} \tag{6}$$

Using Equation 4, we can write

$$\Delta I_{\ell m} = \Delta H_{\ell m} - \frac{4\pi a^3}{M_e}[\rho_i \Delta I_{\ell m} + \rho_w \Delta S_{\ell m}] T_\ell h_\ell \tag{7}$$

Solving for the change in ice thickness gives a final expression:

$$\Delta I_{\ell m} = \left(1 + \frac{4\pi a^3 \rho_i h_\ell T_\ell}{M_e}\right)^{-1}\left[\Delta H_{\ell m} - \frac{4\pi a^3 T_\ell}{M_e}\rho_w \Delta S_{\ell m}\right] \tag{8}$$

In applying this expression to regions proximal to ice cover, it is common to neglect ocean load changes, since they are relatively small. Neglecting this term gives

$$\Delta I_{\ell m} = \left(1 + \frac{4\pi a^3 \rho_i h_\ell T_\ell}{M_e}\right)^{-1} \Delta H_{\ell m} \equiv \alpha_\ell \Delta H_{\ell m} \tag{9}$$

https://doi.org/10.5194/egusphere-2023-2451
Preprint. Discussion started: 17 November 2023

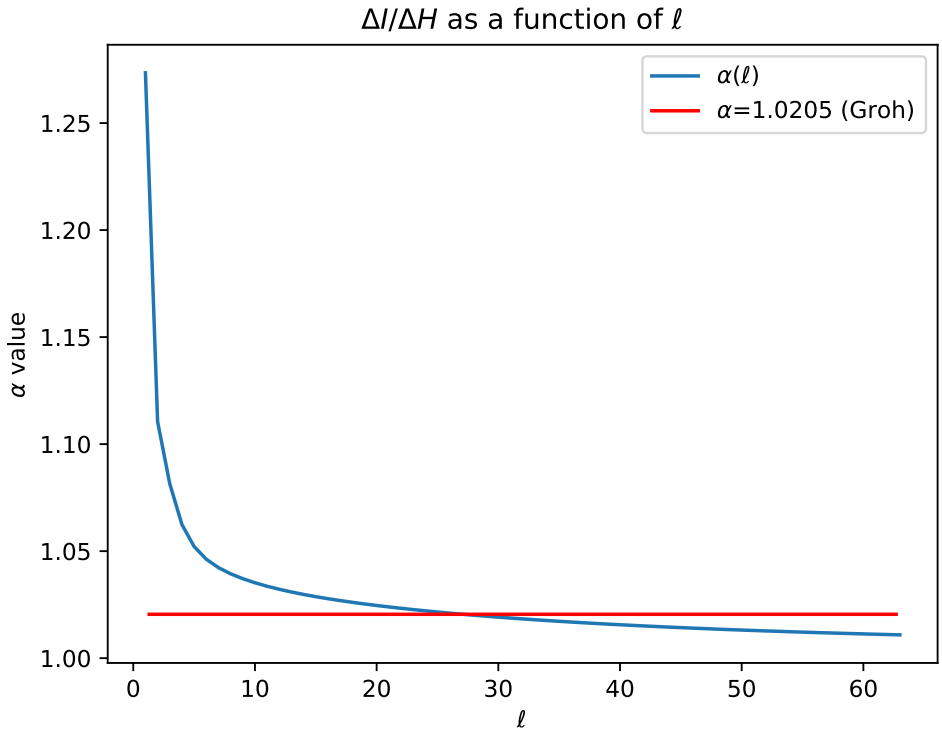

Figure 1. The value of the parameter α_ℓ as a function of the spherical harmonic degree l, as defined in Equation 10. The red line indicates the value of α_ℓ adopted in Groh et al. (2012).

Thus

$$\alpha_\ell = \left(1 + \frac{4\pi a^3 \rho_i h_\ell T_\ell}{M_e}\right)^{-1} \tag{10}$$

This expression indicates that the mapping between ice height and ice thickness changes is dependent on spatial scale (via the degree ℓ), as shown in Figure 1.

Another assumption in the above derivation is that the response of the solid earth to modern ice loss in the Antarctic region can be represented by an elastic Earth model. The inaccuracy this introduces will be a function of the timescale of ice loading that is considered and the viscosity of the underlying mantle. In the results section, we investigate this issue by considering both elastic and viscoelastic Earth models. Our predictions also include the impact of water height changes $\Delta S_{\ell m}$ on the mapping.

3 Methods

In all the calculations presented below, we adopt a specified ice-load history and compute gravitationally self-consistent sea level variations using a Maxwell viscoelastic Earth model. The sea level theory accounts for migration of shorelines and the

https://doi.org/10.5194/egusphere-2023-2451
Preprint. Discussion started: 17 November 2023

feedback of Earth's rotation changes into sea level (Kendall et al., 2005). The solutions are based on a finite volume formulation of the surface loading problem which allows arbitrary, 3D variations in mantle viscoelastic structure (Latychev et al., 2005). The GIA and modern ice mass flux calculations are distinguished by the input ice histories, each of which we discuss in turn.

The GIA simulations adopt three different ice histories: the global ICE-6G_C model of Peltier et al. (2015), the Antarctic model of Ivins and James (2005) (referred to as IJ05), and an ice history derived by coupling a three-dimensional Antarctic ice sheet model with a GIA-based sea level model (hereafter the G18 model) (Gomez et al., 2018). The G18 model is combined with the non-Antarctic components of the global ICE-5G model (Peltier, 2004), while the non-Antarctic components of the ICE-6G_C model are used to create a global model with the IJ05 Antarctic history. Each of these ice histories is coupled to a viscoelastic Earth model. The ICE-6G_C model is paired with the one-dimensional, three-layer VM5a model, in which the viscosity varies from 5×10^{20} Pa s in the upper mantle to 3×10^{21} Pa s in the deep mantle (Peltier et al., 2015). The VM5a model has an elastic lithospheric thickness of 90 km. The three-layer IJ05 model includes a lithospheric thickness of 90 km and mantle viscosities of 4×10^{20} Pa s for the upper mantle, 6×10^{21} Pa s for the lower mantle between 670 km and 1200 km depth, and 8×10^{22} Pa s for the lower mantle between 1200 km depth and the core-mantle boundary (Ivins and James, 2005). The G18 model adopts a three-dimensional Earth model derived by Hay et al. (2017) on the basis of seismic tomographic results (An et al., 2015; Heeszel et al., 2016). The model has a mean lithospheric thickness of 65 km in West Antarctica and 200 km in East Antarctica (Hay et al., 2017). The viscosity beneath West Antarctica reaches values as low as 10^{18} Pa s (see Figure 2), consistent with the tectonic rift setting of the region (Wörner, 1999). The elastic structure for all three models is given by the seismic model PREM (Dziewonski and Anderson, 1981). Note that while we computed present-day uplift rates from the IJ05 and G18 models, we obtained these rates for ICE-6G_C directly from the model's creator.

The calculations of the Earth's response to modern mass flux are based on the fETISH32 (EXP A1) projections to 2055 CE of the Antarctic ice sheet (Pattyn, 2017). The projection is one of ∼180 such projections included in the Ice Sheet Model Intercomparison Project for CMIP6 (ISMIP6) and is characterized by a net global mean sea level rise of 14.7 cm from 2015 to 2055 (the highest GMSL rise of any projection in ISMIP6). We pair this ice projection with three Earth models: a purely elastic Earth model based on PREM and two three-dimensional viscoelastic models: one derived by Austermann et al. (2021) based on results from Richards et al. (2020) (henceforth, the RH20 model) and the model adopted in the G18 simulation mentioned above (Hay et al., 2017). The Richards et al. (2020) model is constrained by seismic tomography (Schaeffer and Lebedev, 2014), laboratory measurements of mantle materials, and seismic attenuation measurements. It is characterized by a shallow mantle viscosity of $\sim 10^{19}$ Pa s below West Antarctica (see Figure 2).

4 Results and Discussion

4.1 GIA Correction to Altimeter Records

Figure 3 shows present-day rates of crustal uplift due to GIA for each ice model: G18, ICE-6G_C, and IJ05. The relative magnitude of the signals is roughly consistent with the excess Antarctic ice volume at LGM in each model: 6 m, 10 m, and 14 m in units of equivalent GMSL for the G18, IJ05, and ICE-6G_C simulations, respectively (Gomez et al., 2018; Ivins

https://doi.org/10.5194/egusphere-2023-2451
Preprint. Discussion started: 17 November 2023

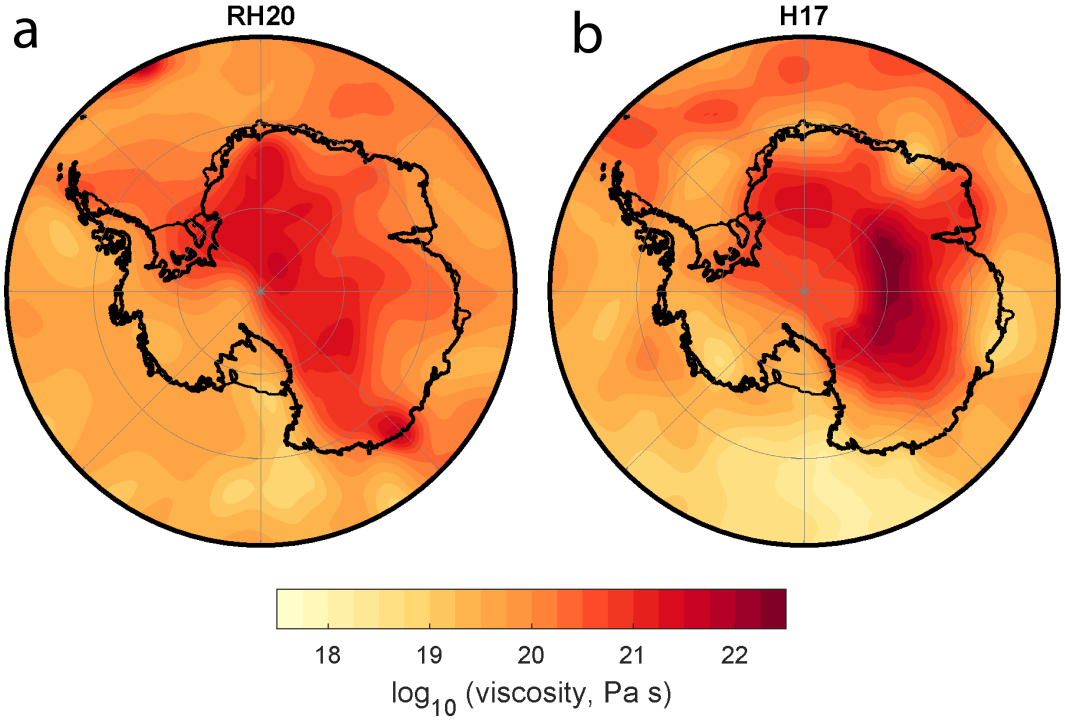

Figure 2. Mean viscosities from the base of the lithosphere to 400 km depth under Antarctica in the two three-dimensional viscoelastic Earth models: (a) from Richards et al. (2020), (b) from Hay et al. (2017). These models are adopted in the calculation of the Earth's response to modern mass flux.

and James, 2005; Peltier et al., 2015). Some of these differences may arise from differing levels of ice mass flux in the late Holocene across models and the resulting elastic response; however, these variations should be small. In the G18 model, the largest rates of uplift are in Oates Land in East Antarctica, where uplift exceeds 10 $\mathrm{mm\,yr^{-1}}$ in a small area), and south of the Ronne Ice Shelf (peak rates of $\sim$ 6 $\mathrm{mm\,yr^{-1}}$). The ICE-6G_C model predicts uplift south of the Ronne Ice Shelf and in Marie Byrd Land, with rates peaking at about 13 $\mathrm{mm\,yr^{-1}}$. The IJ05 model locates its highest uplift rates west of the Ronne Ice Shelf and in Marie Byrd Land, where the rates do not exceed 7 $\mathrm{mm\,yr^{-1}}$.

The difference maps in Figure 4 indicate that the GIA correction and therefore the modern ice thickness changes inferred from the residual (GIA-corrected) uplift signal are subject to significant uncertainty. For example, let us assume that the G18 model, derived from a GIA calculation based on a more realistic, three-dimensional Earth model, and consistent with ice sheet physics, provides the most accurate prediction of uplift rates. Then, the differences in uplift rates in Figure 4 represent a relatively accurate proxy for this uncertainty given that the ratio of uplift rate to ice thickness change is close to 1 for the case of modern ice mass flux (see below). These differences, when integrated over the whole of Antarctica, yield a total ice volume change uncertainty equivalent to 0.028 $\mathrm{mm\,yr^{-1}}$ global mean sea level change for the IJ05 case and 0.046 $\mathrm{mm\,yr^{-1}}$ for the ICE-6G_C case.

https://doi.org/10.5194/egusphere-2023-2451
Preprint. Discussion started: 17 November 2023

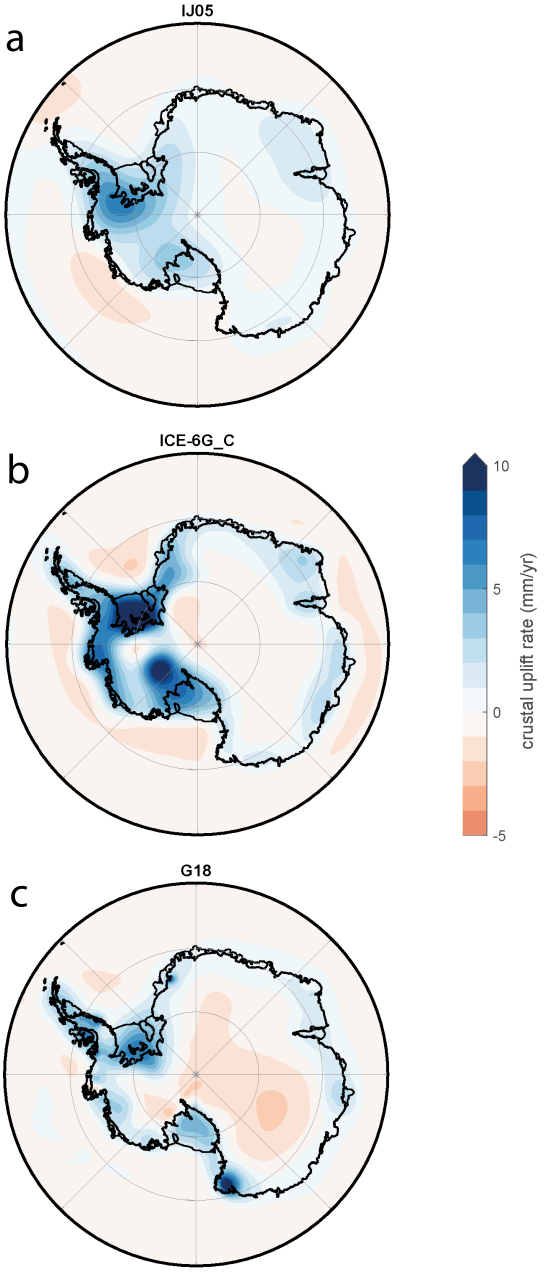

Figure 3. Present-day crustal deformation rates due to GIA computed for three different ice history/Earth model combinations: (a) the IJ05 model from Ivins and James (2005), (b) the ICE-6G_C model from Peltier et al. (2015), and (c) the G18 model from Gomez et al. (2018).

https://doi.org/10.5194/egusphere-2023-2451
Preprint. Discussion started: 17 November 2023

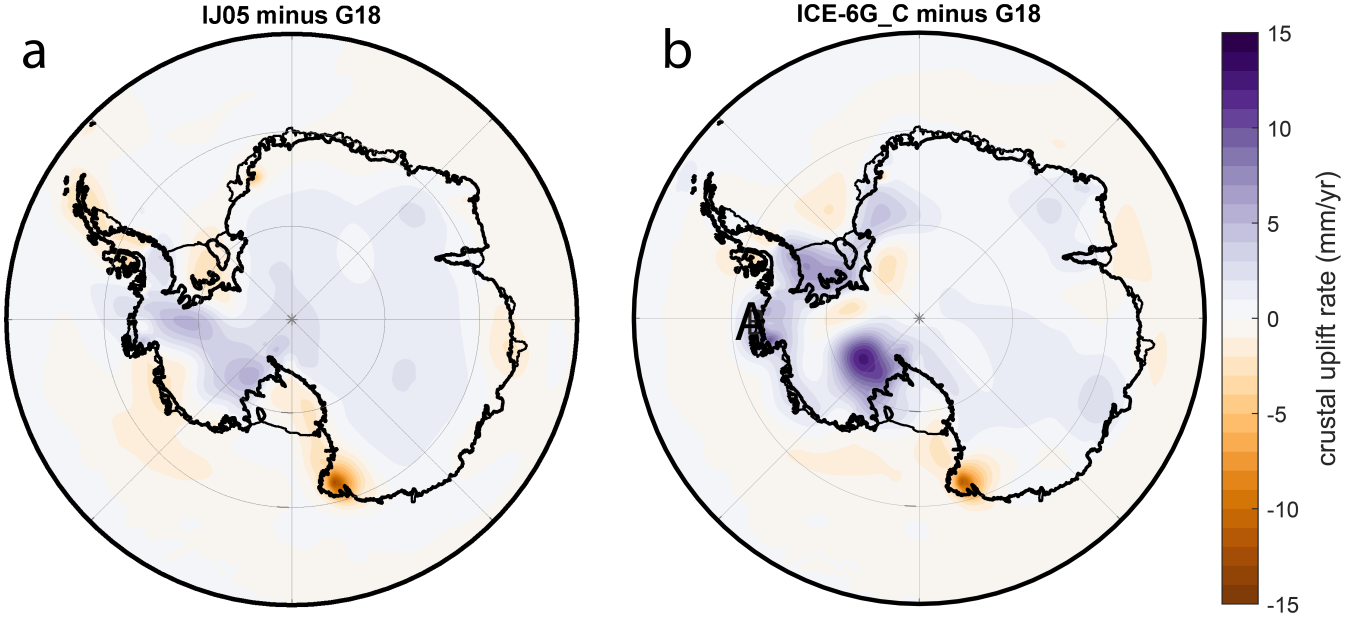

Figure 4. Differences in predicted crustal deformation rates between the G18 model and the IJ05 (a) and ICE-6G_C (b) models.

4.2 Mapping Altimeter Measurements of Ice Height Changes to Thickness Changes

As shown in the theory section, the mapping between ice height and ice thickness changes, α_ℓ, must be dependent on spatial scale but is commonly assumed to be a single scale factor (Groh et al., 2012). To explore the inaccuracy introduced by this assumption, we computed the response of a set of Earth models to the fETISH32 (EXP A1) projection of ice thickness change over the forty years between 2015 and 2055 (Figure 5). The computed ratio between ice thickness and ice height changes in the case of an elastic Earth model and two three-dimensional viscoelastic models - RH20 (Richards et al., 2020) and the earth model adopted in the G18 simulation described above (Figure 2) - is shown in Figure 6. A cutoff of 10 m of ice height change is introduced to focus on the areas of sizeable ice mass flux.

The value of α varies between 0.98 and 1.07 in areas of the Antarctic with at least 10 m of ice height change. The largest changes in this scaling factor occur in regions of high mass flux, such as Pine Island and Thwaites Glaciers. In these two areas, the value of α increases as one moves inland from the coast. There are two reasons for this trend. First, the crustal response at a given site is proportional to the distance-weighted integral of the total load change near that site. Since the change in the ocean load is small close to the coastline relative to the local ice mass flux, the integrated load change a site will experience will tend to increase moving inland (i.e., in contrast to a coastal site, an inland site has ice mass flux on all sides). Second, the spatial scale of ice streams varies with location: the catchment basin tends to narrow as one moves toward the coastline. As indicated in Figure 1, the value of α will be smaller when the characteristic scale of the mass flux (here, the scale of the catchment basin) decreases.

https://doi.org/10.5194/egusphere-2023-2451
Preprint. Discussion started: 17 November 2023

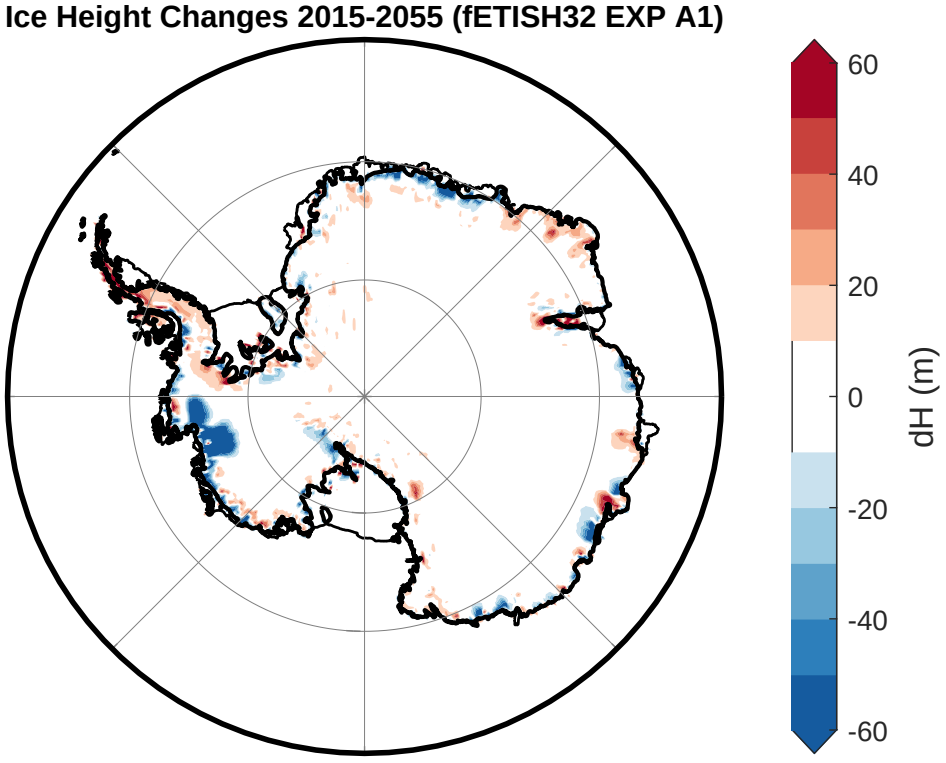

Figure 5. Ice thickness change (meters) 2015-2055 CE from fETISH32 EXP A1.

The introduction of viscous deformation has negligible impact over East Antarctica and parts of West Antarctica that are characterized by relatively high viscosity (Figure 2). The largest impact is once again in the areas of greatest mass flux, near Pine Island and Thwaites Glaciers which overlay regions of relatively low mantle viscosity and where the ratio α_ℓ grows more quickly relative to the elastic case as one moves inland. This trend becomes more pronounced as the shallow viscosity of the underlying Earth model decreases, as it does in these areas as one moves from considering the RH20 model results to the G18 model results.

Using these projections, we can estimate the error in estimates of total ice volume changes that is incurred by assuming the constant value $\alpha = 1.0205$. In the case of the projection based on the RH20 viscoelastic model, applying this assumption would underestimate the ice volume loss in the next 40 years by 50 km^3, 700 km^3, and 400 km^3 in the Antarctic Peninsula, West Antarctica, and East Antarctica, respectively. The analogous values are 30 km^3, 1200 km^3, and 400 km^3 for the G18 model. Summing each triplet yields an underestimate of 3.2 mm and 4.5 mm in units of equivalent GMSL change, respectively, for the RH20 and G18 model projections.

https://doi.org/10.5194/egusphere-2023-2451
Preprint. Discussion started: 17 November 2023

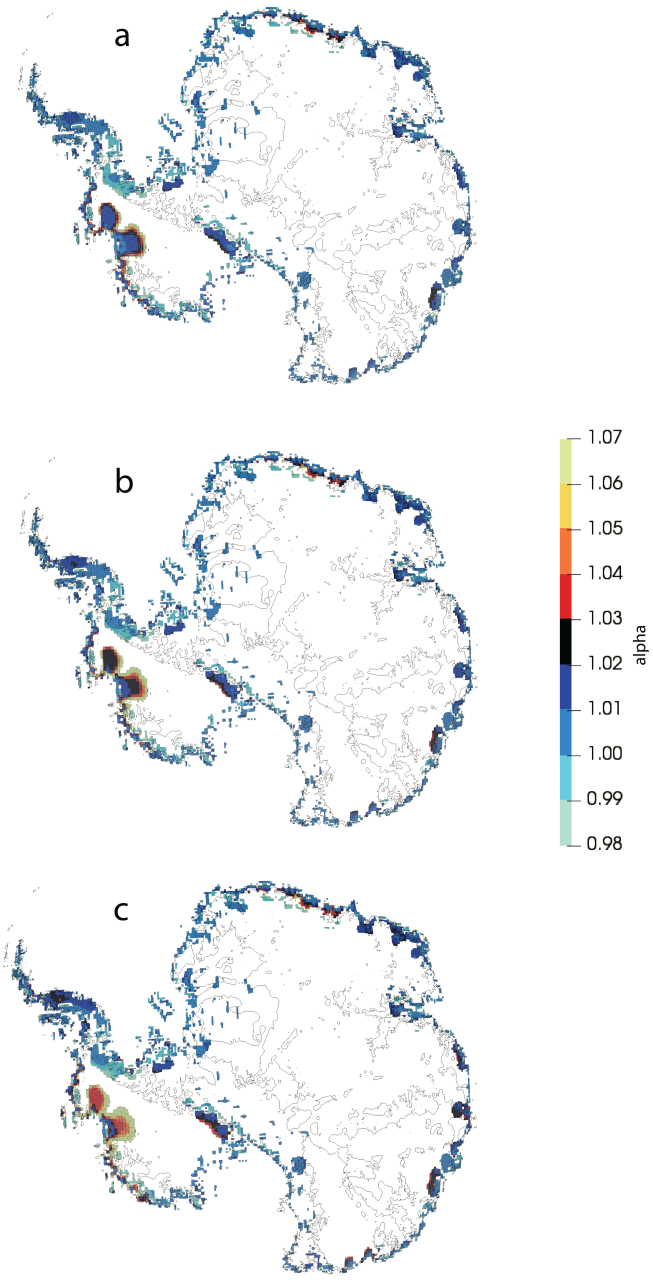

Figure 6. The ratio of ice thickness to ice height changes (α) from 2015 to 2055 in regions with an ice thickness change greater than 10 m. (a) is a map computed by assuming a fully elastic Earth model. (b) and (c) are the corresponding maps based on the Richards et al. (2020) (RH20) and the Hay et al. (2017) (G18) viscoelastic models, respectively.

https://doi.org/10.5194/egusphere-2023-2451
Preprint. Discussion started: 17 November 2023

5 Conclusions

We have investigated potential errors in estimates of ice thickness change inferred from satellite altimetry measurements arising from: 1) errors in the correction for GIA, and 2) the mapping of GIA-corrected ice height changes to ice thickness changes associated with modern melt using a single (i.e., geographically invariant) scalar.

Shepherd et al. (2012) noted that significant uncertainty in the GIA correction to Antarctic ice mass flux estimates is introduced by uncertainty in the excess volume of Antarctic glaciation at LGM. Their analysis adopted the ice history of Whitehouse et al. (2012), which had an excess ice volume significantly smaller than some previous estimates (8 m in units of equivalent GMSL rise). This ice history was paired with a viscosity profile with a preferred range of upper mantle viscosity of $0.8 - 2.0 \times 10^{21}$ $\mathrm{Pa\,s}$. The present analysis has reconsidered this issue using an ice history generated from a coupled ice sheet sea level model and a significantly more realistic viscoelastic mantle model for the region (i.e., the G18 simulation). The latter is characterized by significant variability in viscosity, including low-viscosity zones beneath some sections of the West Antarctic. We find that the differences in the GIA correction between the G18 model and earth model-ice history pairs inferred in recent GIA analysis, when integrated over the Antarctic, map into an uncertainty in total present-day ice volume change of 0.046 $\mathrm{mm\,yr^{-1}}$ GMSL equivalent for the ICE-6G_C case and 0.028 $\mathrm{mm\,yr^{-1}}$ for the IJ05 case. These uncertainties are 12% and 7%, respectively, of the estimated AIS mass loss over the decade 2010-2020 (Velicogna et al., 2020).

Previous studies have scaled GIA-corrected altimeter measurements of ice height changes into thickness changes using a single scaling close to 1.02 (Groh et al., 2012). The true scaling will depend on both the spatial scale of the loading and also on the rheological properties of the underlying crust and mantle. We have found, using calculations based on a projection of Antarctic mass flux over the next 40 years, that this scaling can vary by $\sim$10% (between 0.98 and 1.07). The error incurred in estimates of ice volume changes based on this constant scaling when considering published projections of modern Antarctic melt is up to 4 mm GMSL equivalent over the next 40 years (approximately 3% of the total Antarctic contribution over this time frame in the adopted ice sheet projection fETISH32, EXP A1).

Data availability. The ice histories adopted in this study are taken from published sources.

Author contributions. All authors have made substantial contributions to this article (N.V.: formal analysis, investigation, visualization, writing – original draft, writing – review and editing. L.P.: methodology, writing – review and editing. K.L.: methodology, software, validation, writing – review and editing. N.G.: conceptualization, writing – review and editing. E.P.: conceptualization, writing – review and editing. J.X.M.: conceptualization, supervision, writing – review and editing) and have approved the final version of the manuscript.

Competing interests. The authors declare that they have no competing interests.

https://doi.org/10.5194/egusphere-2023-2451
Preprint. Discussion started: 17 November 2023

Acknowledgements. This material is based upon work supported by Harvard University [N.V., L.P., J.X.M], NSF awards 134341 and 134347 [N.V., L.P., J.X.M], the Fonds de Recherche du Québec-Nature et technologies [L.P.], Natural Sciences and Engineering Research Council of Canada Postgraduate Scholarships - Doctoral Program [L.P.], Star-Friedman Challenge [L.P.], Natural Sciences and Engineering Research Council of Canada Grant No. RGPIN-2016-05159 [N.G.], Canada Research Chairs Program Grant No. 241814 [N.G.], NASA award 80NSSC21K1790 [E.P.], and the John D. and Catherine T. MacArthur Foundation [J.X.M.].

https://doi.org/10.5194/egusphere-2023-2451
Preprint. Discussion started: 17 November 2023

References

An, M., Wiens, D. A., Zhao, Y., Feng, M., Nyblade, A., Kanao, M., Li, Y., Maggi, A., and Lévêque, J.-J.: Temperature, lithosphere-asthenosphere boundary, and heat flux beneath the Antarctic Plate inferred from seismic velocities, Journal of Geophysical Research: Solid Earth, 120, 8720–8742, https://doi.org/10.1002/2015JB011917, 2015.

Austermann, J., Hoggard, M. J., Latychev, K., Richards, F. D., and Mitrovica, J. X.: The effect of lateral variations in Earth structure on Last Interglacial sea level, Geophysical Journal International, 227, 1938–1960, https://doi.org/10.1093/gji/ggab289, 2021.

Dziewonski, A. M. and Anderson, D. L.: Preliminary reference Earth model, Physics of the Earth and Planetary Interiors, 25, 297–356, https://doi.org/10.1016/0031-9201(81)90046-7, 1981.

Farrell, W. E. and Clark, J. A.: On Postglacial Sea Level, Geophysical Journal International, 46, 647–667, https://doi.org/10.1111/j.1365-246X.1976.tb01252.x, 1976.

Gomez, N., Pollard, D., and Mitrovica, J. X.: A 3-D coupled ice sheet – sea level model applied to Antarctica through the last 40 ky, Earth and Planetary Science Letters, 384, 88–99, https://doi.org/10.1016/j.epsl.2013.09.042, 2013.

Gomez, N., Latychev, K., and Pollard, D.: A Coupled Ice Sheet–Sea Level Model Incorporating 3D Earth Structure: Variations in Antarctica during the Last Deglacial Retreat, Journal of Climate, 31, 4041–4054, https://doi.org/10.1175/JCLI-D-17-0352.1, 2018.

Groh, A., Ewert, H., Scheinert, M., Fritsche, M., Rülke, A., Richter, A., Rosenau, R., and Dietrich, R.: An investigation of Glacial Isostatic Adjustment over the Amundsen Sea sector, West Antarctica, Global and Planetary Change, 98-99, 45–53, https://doi.org/10.1016/j.gloplacha.2012.08.001, 2012.

Hay, C. C., Lau, H. C. P., Gomez, N., Austermann, J., Powell, E., Mitrovica, J. X., Latychev, K., and Wiens, D. A.: Sea Level Fingerprints in a Region of Complex Earth Structure: The Case of WAIS, Journal of Climate, 30, 1881–1892, https://doi.org/10.1175/JCLI-D-16-0388.1, 2017.

Heeszel, D. S., Wiens, D. A., Anandakrishnan, S., Aster, R. C., Dalziel, I. W. D., Huerta, A. D., Nyblade, A. A., Wilson, T. J., and Winberry, J. P.: Upper mantle structure of central and West Antarctica from array analysis of Rayleigh wave phase velocities, Journal of Geophysical Research: Solid Earth, 121, 1758–1775, https://doi.org/10.1002/2015JB012616, 2016.

Ivins, E. R. and James, T. S.: Antarctic glacial isostatic adjustment: a new assessment, Antarctic Science, 17, 541–553, https://doi.org/10.1017/S0954102005002968, 2005.

Kendall, R. A., Mitrovica, J. X., and Milne, G. A.: On post-glacial sea level - II. Numerical formulation and comparative results on spherically symmetric models, Geophysical Journal International, 161, 679–706, https://doi.org/10.1111/j.1365-246X.2005.02553.x, 2005.

Lambeck, K., Rouby, H., Purcell, A., Sun, Y., and Sambridge, M.: Sea level and global ice volumes from the Last Glacial Maximum to the Holocene, Proceedings of the National Academy of Sciences, 111, https://doi.org/10.1073/pnas.1411762111, 2014.

Latychev, K., Mitrovica, J. X., Tromp, J., Tamisiea, M. E., Komatitsch, D., and Christara, C. C.: Glacial isostatic adjustment on 3-D Earth models: a finite-volume formulation, Geophysical Journal International, 161, 421–444, https://doi.org/10.1111/j.1365-246X.2005.02536.x, 2005.

Li, T., Wu, P., Wang, H., Steffen, H., Khan, N. S., Engelhart, S. E., Vacchi, M., Shaw, T. A., Peltier, W. R., and Horton, B. P.: Uncertainties of Glacial Isostatic Adjustment Model Predictions in North America Associated With 3D Structure, Geophysical Research Letters, 47, https://doi.org/10.1029/2020GL087944, 2020.

Mitrovica, J. X. and Milne, G. A.: On the origin of late Holocene sea-level highstands within equatorial ocean basins, Quaternary Science Reviews, 21, 2179–2190, https://doi.org/10.1016/S0277-3791(02)00080-X, 2002.

https://doi.org/10.5194/egusphere-2023-2451
Preprint. Discussion started: 17 November 2023

Pattyn, F.: Sea-level response to melting of Antarctic ice shelves onmulti-centennial time scales with the fast ElementaryThermomechanical Ice Sheet model (f.ETISh v1.0), preprint, Numerical Modelling, https://doi.org/10.5194/tc-2017-8, 2017.

Peltier, W.: Global glacial isostasy and the surface of the ice-age Earth: the ICE-5G (VM2) model and GRACE, Apr Annu. Rev. Earth Planet. Sci, 20, 111–149, https://doi.org/10.1146/annurev.earth.32.082503.144359, 2004.

Peltier, W., Argus, D. F., and Drummond, R.: Space geodesy constrains ice age terminal deglaciation: The global ICE-6G_C (VM5a) model, Journal of Geophysical Research: Solid Earth, 120, 450–487, https://doi.org/10.1002/2014JB011176, 2015.

Powell, E., Gomez, N., Hay, C., Latychev, K., and Mitrovica, J. X.: Viscous Effects in the Solid Earth Response to Modern Antarctic Ice Mass Flux: Implications for Geodetic Studies of WAIS Stability in a Warming World, Journal of Climate, 33, 443–459, https://doi.org/10.1175/JCLI-D-19-0479.1, publisher: American Meteorological Society Section: Journal of Climate, 2020.

Richards, F. D., Hoggard, M. J., White, N., and Ghelichkhan, S.: Quantifying the Relationship Between Short-Wavelength Dynamic Topography and Thermomechanical Structure of the Upper Mantle Using Calibrated Parameterization of Anelasticity, Journal of Geophysical Research: Solid Earth, 125, https://doi.org/10.1029/2019JB019062, 2020.

Schaeffer, A. J. and Lebedev, S.: Imaging the North American continent using waveform inversion of global and USArray data, Earth and Planetary Science Letters, 402, 26–41, https://doi.org/10.1016/j.epsl.2014.05.014, 2014.

Shepherd, A., Ivins, E. R., A, G., Barletta, V. R., Bentley, M. J., Bettadpur, S., Briggs, K. H., Bromwich, D. H., Forsberg, R., Galin, N., Horwath, M., Jacobs, S., Joughin, I., King, M. A., Lenaerts, J. T. M., Li, J., Ligtenberg, S. R. M., Luckman, A., Luthcke, S. B., McMillan, M., Meister, R., Milne, G., Mouginot, J., Muir, A., Nicolas, J. P., Paden, J., Payne, A. J., Pritchard, H., Rignot, E., Rott, H., Sørensen, L. S., Scambos, T. A., Scheuchl, B., Schrama, E. J. O., Smith, B., Sundal, A. V., van Angelen, J. H., van de Berg, W. J., van den Broeke, M. R., Vaughan, D. G., Velicogna, I., Wahr, J., Whitehouse, P. L., Wingham, D. J., Yi, D., Young, D., and Zwally, H. J.: A Reconciled Estimate of Ice-Sheet Mass Balance, Science, 338, 1183–1189, https://doi.org/10.1126/science.1228102, 2012.

Velicogna, I., Mohajerani, Y., A, G., Landerer, F., Mouginot, J., Noel, B., Rignot, E., Sutterley, T., van den Broeke, M., van Wessem, M., and Wiese, D.: Continuity of Ice Sheet Mass Loss in Greenland and Antarctica From the GRACE and GRACE Follow-On Missions, Geophysical Research Letters, 47, https://doi.org/10.1029/2020GL087291, 2020.

Whitehouse, P. L., Bentley, M. J., Milne, G. A., King, M. A., and Thomas, I. D.: A new glacial isostatic adjustment model for Antarctica: calibrated and tested using observations of relative sea-level change and present-day uplift rates, Geophysical Journal International, 190, 1464–1482, https://doi.org/10.1111/j.1365-246X.2012.05557.x, 2012.

Wörner, G.: Lithospheric dynamics and mantle sources of alkaline magmatism of the Cenozoic West Antarctic Rift System, Global and Planetary Change, 23, 61–77, https://doi.org/10.1016/S0921-8181(99)00051-X, 1999.